Two dimensional incompressible unsteady nanofluid flow over a stretching sheet by porous medium with the impact of thermal stratification, solutal stratification and non-uniform heat generation/absorption

Y. Raja Obula Reddy
Department of mathematics
Rajeev Gandhi Memorial College of Engineering and Technology, Nandyal-518501, Andhra Pradesh, India.
Email ID: rajaobulareddy@mail.com

Abstract: In this paper, the influence of thermal stratification, solutal stratification on unsteady nanofluid flow over a stretching sheet by porus porous medium with non-uniform heat source/sink was analyzed numerically. By using similarity transformations nonlinear partial differential equations are reduced into ordinary differential equations and are solved by Finite element method. Impact of different parameters, such as, magnetic parameter (0.1 – 1.0), buoyancy ratio parameter (0.1 – 4.5), radiation parameter (0.5 – 1.7), Rayleigh number (0.1 – 0.7), thermophoresis parameter (0.4 – 1.5), thermal stratification parameter (0.01 – 1.0), Brownian motion parameter (1.0 – 2.0), solutal stratification parameter (0.01 – 1.0), unsteadiness parameter (0.1 – 0.4), space – dependent (-0.5 – 0.4) and temperature dependent (-0.5 – 0.2) heat source/sink parameters on velocity, temperature and concentration profiles is calculated and are illustrated graphically. Skin-friction coefficient, Nusselt and Sherwood number are calculated and the results are shown in tabular form. It is found that the thermal stratification parameter get worse the temperature of the fluid. The concentration of the fluid decreases with rising values of solutal stratification parameter. The thermal boundary layer thickness elevates with higher values of Brownian motion and thermo phoresis parameters.

Keywords: **Nanofluid, Unsteady, Porous medium, Stratification, Non-uniform heat sorce/sink.**

1. Introduction

The thermal and mechanical properties of materials have become the rapid growth of interest in recent years because of its extensive range of applications in scientific and engineering communities, such as, semiconductors, transistors, solar storage, heat exchangers, cooling systems, evaporators, etc., Conventional heat transfer fluids like water, kerosene, ethylene glycol, oils etc., have low heat transfer capabilities due to their limited thermal conductivity. Various methods have been incorporated to enhance the thermal conductivity of these fluids. By suspending nanometer sized (1 – 100 nm) particles, called nanoparticles, into the base fluids we increase its thermal conductivity and the resulting fluid is known as nanofluid. These nanofluids have no additional issues of destruction, sedimentation, non – Newtonian properties and extra pressure drop. Keeping above applications first "Choi [1]." discussed the thermal conductivity enhancement of fluids by adding nanoparticles while doing research work on new coolants and cooling technologies. Several authors ("Eastman et al. [2]", "Buongiorno, [3]", "Abu-Nada et al. [4]", "Kuznetsov et al. [5]") have discussed about the natural convection heat transfer enhancement of various nanoparticles.

The boundary layer heat and mass transfer flow over a stretching sheet has many practical applications such as extrusion of polymer, cooling of metallic plate, drawing plastic sheet and films, paper production, glass blowing etc., In the above applications the quality of the final product depends on the heat transfer rate between the stretching surface and the fluid during the cooling or heating process. Also, the motion of stretched sheet may start spontaneously from relaxation. Therefore, the choice of a suitable cooling/heating liquid is essential as it has a direct impact on the rate of heat transfer. The unsteady flow and heat transfer occur when a flat plate is stretched suddenly. Magneto nanofluids have specific applications in biomedicine, optical modulators, magnetic cell separation, magneto-optical wavelength filters, silk float separation, nonlinear optical materials, hyperthermia, optical switches, drug delivery, optical gratings etc. Magneto nanofluids are useful to guide the particles up the blood stream to a tumor with magnets. This is due to the fact that the magnetic nanoparticles are regarded more adhesive to tumor cells than non-malignant cells. Such particles absorb more power than microparticles in alternating current magnetic fields tolerable in humans i.e. for cancer therapy. "Hamad [6]" examined the impact of magnetic field and nanoparticle volume fraction on natural convection flow and heat transfer analysis of four varieties of nanofluids (Cu – water, Ag – water, Al_2O_3 – water and TiO_2 – water) over a linear stretching sheet and found depreciation in the rates heat transfer with higher values of nanoparticle volume fraction parameter. "Noghrehabadi et al. [7]." have analyzed nanofluid flow over stretching sheet by taking velocity slip and nanoparticle volume fractions into the account. They reported increment in the thickness of thermal boundary layer as the values of velocity slip parameter raises. "Rana et al. [8]." studied the numerical solution to the heat transfer characteristics of nanofluid over a nonlinearly stretching sheet. "Noghrehabadi et al. [9]." have deliberated the influence of convective boundary condition and partial slip on nanofluid flow over stretching sheet. "Chamkha et al.

 https://doi.org/10.37896/pd93.4/93412

[10].” perceived nanofluid flow over a vertical plate embedded in porous medium with heat generation/absorption and found remarkable enhancement in velocity and temperature with rising values of Brownian motion parameter. “Rashidi et al. [11].” have discussed the heat transfer enhancement of nanofluid over stretching sheet with magnetic field and thermal radiation. “Sheikholeslami et al. [12].” presented the flow and heat transfer behavior over a stretching sheet filled with nanofluid saturated porous medium. “Mansur et al. [13].” have deliberated three – dimensional flow of nanofluid over a permeable exponentially stretching/shrinking sheet. “Zaraki et al. [14].” have presented the natural convection heat transfer enhancement of nanofluid over a vertical plate influenced by various aspects of the nanofluid like size, shape, type of added nanoparticles and temperature and type of base fluid. They concluded that the rate of heat transfer is more when the size of added nanoparticles is less, however, the heat transfer enhancement is less when the temperature of the base fluid increases. “Zargartalebi et al. [15].” perceived the impact of Brownian motion and thermophoresis on flow and heat transfer over a stretching sheet under the enhanced boundary conditions with variable thermophysical properties. They found the profiles of nanoparticle volume fraction depreciate with rising values of thermophoretic parameter. “Sheremet et al. [16].” studied the impact of volume fraction parameter of nanoparticles on heated square porous cavity filled with aluminum foam – water based nanofluid and reported significant heat transfer enhancement when the values of Rayleigh number increased from 10 to 1000. “Ismael et al. [17].” investigated the entropy generation on square porous cavity filled with CuO – water based nanofluid and noted that the added CuO nanoparticles remarkably enhances the heat transfer coefficient when the values of Rayleigh number $Ra \geq 100$. “Raja Obula Reddy et al. [18].” examined the effect of magnetic parameter and thermal radiation on boundary layer flow, heat and mass transfer of nanofluidover a horizontal circular cylinder embedded in a porous medium. In this study they observed that the rates of heat transfer worsen, whereas, the rates of mass transfer enhance with higher values of Brownian motion parameter in the boundary layer region.“Hayat et al. [19].” have analyzed the effect of Joule heating and viscous dissipation on Cu - water nanofluid flow over a stretching sheet and noticed remarkable enhancement in the temperature of the fluid as the volume fraction of Cu nanoparticle rises.“Bachok et al. [20].” have discussed the flow and heat transfer characteristics of unsteady boundary layer flow over a stretching/shrinking sheet filled with nanofluid saturated porous medium. “Khalili et al. [21].” perceived unsteady nanofluid flow over a stretching/shrinking sheet saturated by porous medium. The unsteady heat and mass transfer characteristics of nanofluid flow over different geometries studied by several authors (“Makinde et al. [22]”, “Das et al. [23]”, “Pop et al. [24]”, “Ahmada Omar Ali et al. [25]”).

The above literature review reveals that there are no studies that investigate the influence of magnetic field and double stratification on heat and mass transfer characteristics of nanofluid over a stretching sheet through porous media. The problem discussed in this study has immediate applications in solar thermal system, purification system, health care materials, thermal conductors etc.

2. Formulation of the problem

We consider the two-dimensional, incompressible, unsteady nanofluid flow over a stretching sheet saturated by porous medium with the impact of thermal stratification, solutal stratification and non-uniform heat source/sink. The coordinate system is such that x-axis is taken along the stretching surface in the direction of the motion and y-axis is perpendicular to the surface of the sheet as shown schematically in Fig. 1. A uniform magnetic field B_0 is applied along the $\mathrm{y}-\mathrm{axis}$. The surface of the sheet is maintained at uniform temperature $T_w = T_0 + \frac{Ax}{1-at}$ and concentration $C_w = C_0 + \frac{Dx}{1-at}$ and these values are assumed to be greater than the ambient temperature stratified in the form $T_\infty = T_0 + \frac{Bx}{1-at}$ and concentration stratified in the form $C_\infty = C_0 + \frac{Ex}{1-at}$. In the present analysis the nanoparticles are persuaded in the base fluid according to the Brownian motion and thermophoresis. Under the above assumptions and by considering the works of (“Hayat et al. [26]”) the governing equations represent the continuity, momentum, energy and concentration take the following form:

 https://doi.org/10.37896/pd93.4/93412

ISSN: 0369-8963

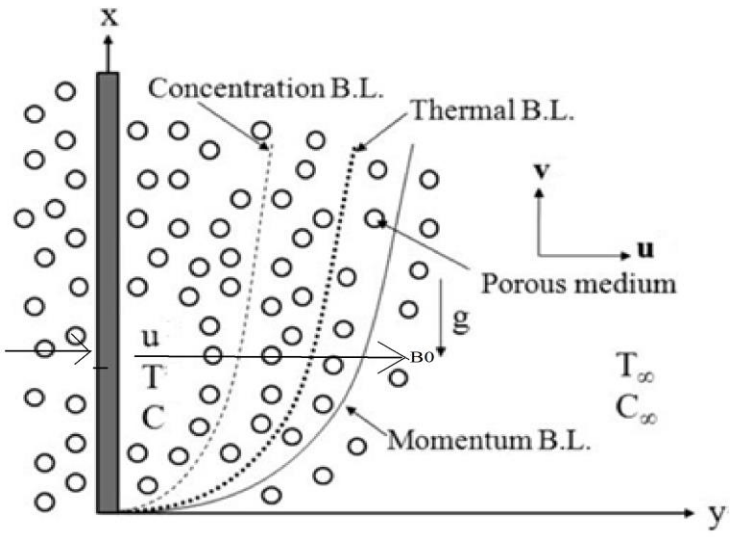

Fig.1. Physical model of the problem.

$$\frac{\partial u}{\partial x}+\frac{\partial v}{\partial y}=0 \quad (1)$$

$$\frac{\partial u}{\partial t}+u\frac{\partial u}{\partial x}+v\frac{\partial u}{\partial y}=\nu\frac{\partial^2 u}{\partial y^2}-\frac{\mu}{\rho k}u+g\left[(1-C_\infty)\beta_T(T-T_\infty)-\frac{(\rho^*-\rho)}{\rho}(C-C_\infty)\right]-\frac{\sigma {B_0}^2}{\rho_f}u \quad (2)$$

$$\frac{\partial T}{\partial t}+u\frac{\partial T}{\partial x}+v\frac{\partial T}{\partial y}=\alpha\frac{\partial^2 T}{\partial y^2}+\tau\left[D_B\frac{\partial C}{\partial y}.\frac{\partial T}{\partial y}+\left(\frac{D_T}{T_\infty}\right)\left(\frac{\partial T}{\partial y}\right)^2\right]-\frac{1}{\rho c_p}\frac{\partial q_r}{\partial y}+\frac{1}{\rho c_p}q''' \quad (3)$$

$$\frac{\partial C}{\partial t}+u\frac{\partial C}{\partial x}+v\frac{\partial C}{\partial y}=D_B\frac{\partial^2 C}{\partial y^2}+\left(\frac{D_T}{T_\infty}\right)\frac{\partial^2 T}{\partial y^2} \quad (4)$$

The associated boundary conditions are

$$u=U=\frac{bx}{1-at},\ v=0,\ T=T_w=T_0+\frac{Ax}{1-at},\quad C=C_w=C_0+\frac{Dx}{1-at},\quad at\ y=0 \quad (5)$$

$$u\to 0,\quad T\longrightarrow T_\infty=T_0+\frac{Bx}{1-at},\quad C\longrightarrow C_\infty=C_0+\frac{Ex}{1-at},\quad at\ y\to\infty \quad (6)$$

The radiative heat flux q_r (using Rosseland approximation) is defined as

$$q_r=-\frac{4\sigma^*}{3K^*}\frac{\partial T^4}{\partial y}, \quad (7)$$

We assume that the temperature variances inside the flow are such that the term T^4 can be represented as linear function of temperature, so, it has Taylor series expansion. After neglecting higher-order terms from the Taylor series expansion of T^4 about T_∞, we get

$$T^4\cong 4{T_\infty}^3T-3{T_\infty}^4. \quad (8)$$

Thus substituting Eq. (8) in Eq. (7), we get

$$q_r=-\frac{16{T_\infty}^3\sigma^*}{3K^*}\frac{\partial T}{\partial y}. \quad (9)$$

The non-uniform heat source/sink, q''', is defined as

$$q'''=\frac{k_{nf}a}{\nu_f}[A^*(T_w-T_\infty)f'+B^*(T-T_\infty)] \quad (10)$$

where A^* and B^* are the coefficients of space and temperature-dependent heat source/sink, respectively. The case $A^*>0, B^*>0$ corresponds to internal heat source and the case $A^*<0, B^*<0$ corresponds to internal heat sink. The following similarity variables are introduced to simplify the mathematical analysis of the problem

$$\eta=\sqrt{\frac{b}{\nu(1-at)}}\,y,\ u=\frac{bx}{1-at}f'(\eta),\ v=-\sqrt{\frac{\nu b}{1-at}}\,f(\eta),\ \theta(\eta)=\frac{T-T_\infty}{T_w-T_0},\ \phi(\eta)=\frac{C-C_\infty}{C_w-C_0}. \quad (11)$$

Substituting Eqns. (9) and (10) into Eqns. (2) – (4), we obtain

$$f'''+ff''-f'^2-\tau\left(f'+\frac{1}{2}\eta f''\right)-(M+K)f'+Ra\,(\theta+Nr\,\phi)=0 \quad (12)$$

$$\frac{1}{Pr}(1+R)\theta''+(f\,\theta'-f'\theta)-\tau\left(S_t+\theta+\frac{1}{2}\eta\,\theta'\right)-S_t f'+Nb\theta'\phi'+Nt\,(\theta')^2+(A1\,f'+B1\,\theta)=0 \quad (13)$$

$$\phi''-Sc\,(f\,\phi'-f'\phi)-Sc\,S_m f'-Sc\ \tau\left(S_m+\phi+\frac{1}{2}\eta\,\phi'\right)+\left(\frac{Nt}{Nb}\right)\theta''=0 \quad (14)$$

 https://doi.org/10.37896/pd93.4/93412

ISSN: 0369-8963

The boundary conditions take the form

$$f = 0, \quad f' = 1, \quad \theta = 1 - S_t, \quad \phi = 1 - S_m, \qquad at \quad \eta = 0, \tag{15}$$

$$f' \longrightarrow 0, \qquad \theta \longrightarrow 0, \qquad \phi \longrightarrow 0, \qquad at \quad \eta \longrightarrow \infty. \tag{16}$$

where prime denotes differentiation with respect to η, and the significant thermophysical parameters dictating the flow dynamics are defined by

$$Nr = \frac{(\rho^* - \rho)(C_w - C_0)}{\rho \beta_T (T_w - T_0)(1 - C_\infty)}, \quad K = \frac{\mu}{\rho\, b\, k}, \quad Pr = \frac{\nu}{\alpha}, \quad R = \frac{16 T_\infty^{\,3} \sigma^*}{3kK^*}, \quad M = \frac{\sigma \beta_0^2}{\rho\, b},$$

$$Sc = \frac{\nu}{D_B}, \quad \tau = \frac{a}{b}, \quad Ra = \frac{(1 - C_\infty) g \beta_T (T_w - T_0)}{b^2 x}, \quad Nb = \frac{\tau D_B (C_w - C_0)}{\nu}, \quad Nt = \frac{\tau\, D_T (T_w - T_0)}{\nu T_\infty},$$

$$S_t = \frac{B}{A}, \qquad A1 = \frac{A^* k (T_w - T_\infty)}{A\, b\, x^2 \rho\, c_p \nu}, \qquad B1 = \frac{B^* k (T_w - T_\infty)}{A\, b\, x^2 \rho\, c_p \nu}, \qquad S_m = \frac{E}{D}.$$

Quantities of practical interest in this problem are skin-friction coefficient (C_f), local Nusselt number (Nu_x), and the local Sherwood number (Sh_x), which are defined as

$$C_f = \frac{\tau_w}{\rho U^2}, \quad Nu_x = \frac{x q_w}{k(T_w - T_\infty)}, \quad Sh_x = \frac{x J_w}{D_B (C_w - C_\infty)} \tag{17}$$

Where the surface shear stress τ_w, wall heat flux q_w and wall mass flux J_w are given by

$$\tau_w = \mu \left(\frac{\partial u}{\partial y}\right)_{y=0}, \; q_w = -\left(k + \frac{16 T_\infty^{\,3} \sigma^*}{3K^*}\right)\left(\frac{\partial T}{\partial y}\right)_{y=0}, \; J_w = -D_B \left(\frac{\partial C}{\partial y}\right)_{y=0} \tag{18}$$

By using above equations we get

$$C_f (Re_x)^{1/2} = f''(0), \quad Nu_x (Re_x)^{-1/2} = -(1 + R)\left(\frac{1}{1 - S_t}\right)\theta'(0),$$

$Sh_x (Re_x)^{-1/2} = -\left(\frac{1}{1 - S_m}\right)\phi'(0)$. Where $Re_x = \frac{Ux}{\nu}$ is the local Reynolds number.

3. Numerical method of Solution

The equations (12) – (14) are extremely non-linear, so finite-element method ("Puneet Rana et al. [27]", "Sudarsana Reddy et al. [28],[29]", "Sudarsana Reddy et al. [30]") has been implemented to solve these non-linear equations.

4. Results and Discussion

The numerical solution is performed and the results are elucidating graphically from Figs. 2 – 30 to know the impact of various parameters on the velocity, temperature and concentration fields.

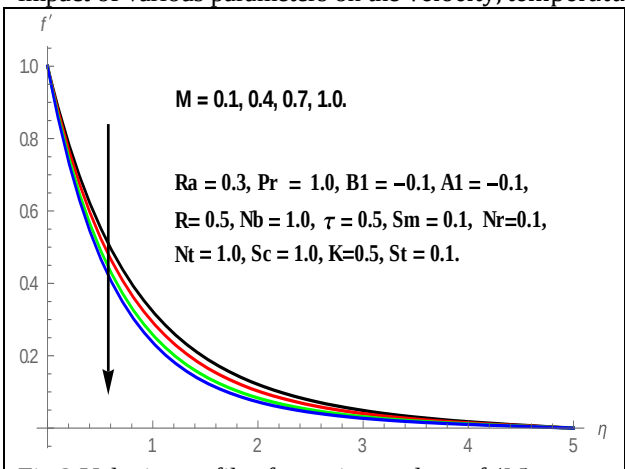

Fig.2.Velocity profiles for various values of (*M*)

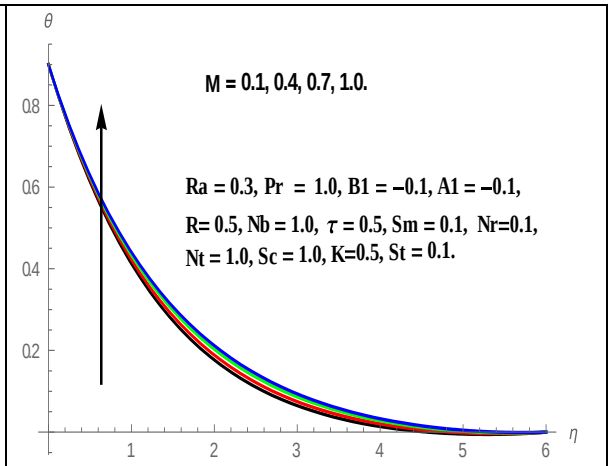

Fig.3.Temperature profiles for various values of (*M*)

https://doi.org/10.37896/pd93.4/93412

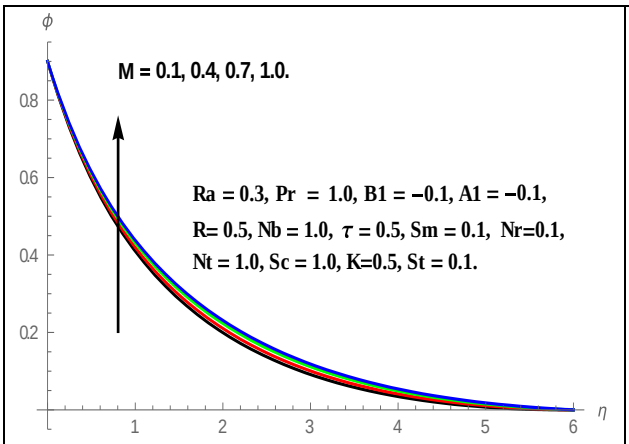

Fig.4.Concentration profiles for various values of (*M*)

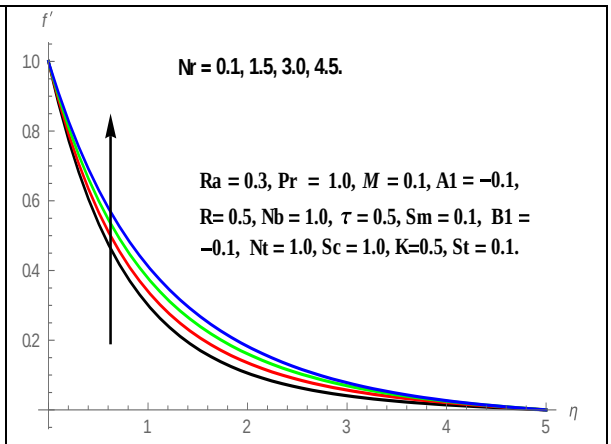

Fig.5.Velocity profiles for various values of (Nr)

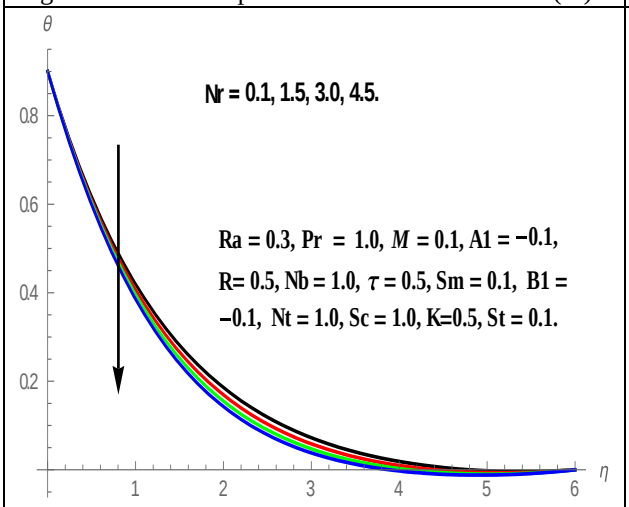

Fig.6.Temperature profiles for various values of (Nr)

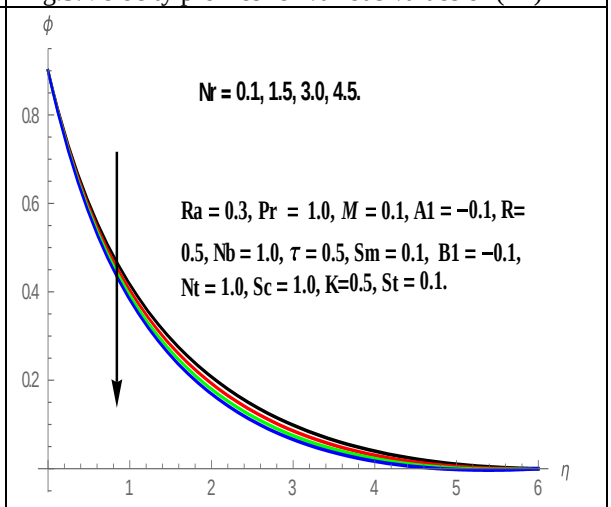

Fig.7.Concentration profiles for various values of (Nr)

The sway of magnetic field parameter (M) on velocity, temperature and concentration profiles is elucidated in Figs. 2 – 4. The velocity profiles of the fluid deteriorate in the boundary layer region as the values of (M) rises (Fig. 2). The thickness of the thermal boundary layer enhances with increase in the values of (M). The reason for this is that Lorentz force enhances the frictional resistance which improves the temperature of the fluid (Fig. 3). Furthermore, the concentration profiles upsurges with higher values of (M) and is shown in Fig. 4.

Figures 5 – 7 depicts the effect of buoyancy ratio parameter (Nr) on velocity, temperature and concentration distributions through the boundary layer regime. It is perceived form Fig. 5 that the hydrodynamic boundary layer thickness is boosted with enhancing values of (Nr). The temperature profiles of the fluid deteriorated with growing values of (Nr) in the boundary layer regime (Fig. 6). The concentration profiles also diminish throughout the fluid region for different improving values of (Nr) as shown in Fig. 7.

https://doi.org/10.37896/pd93.4/93412

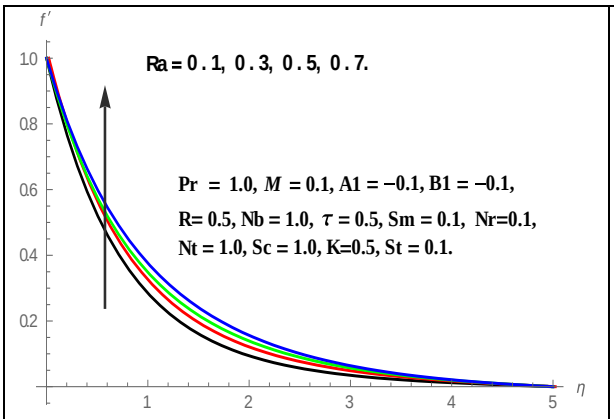

Fig.8. Velocity profiles for various values of (Ra)

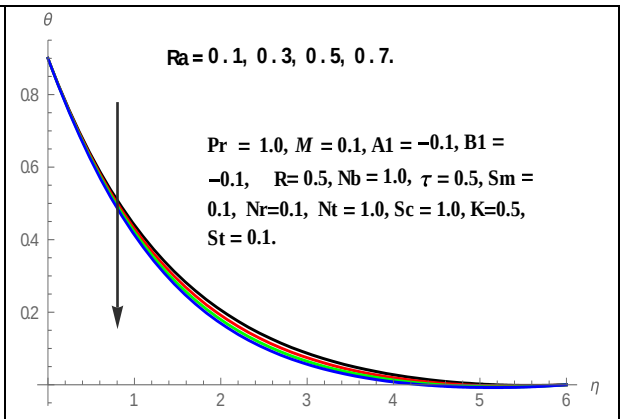

Fig.9. Temperature profiles for various values of (Ra)

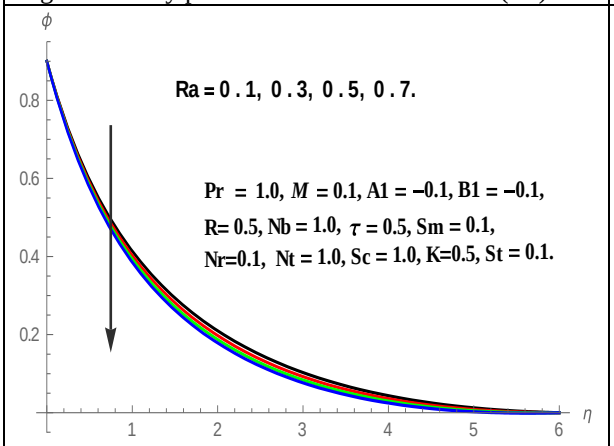

Fig.10.Concetration profiles for various values of (Ra)

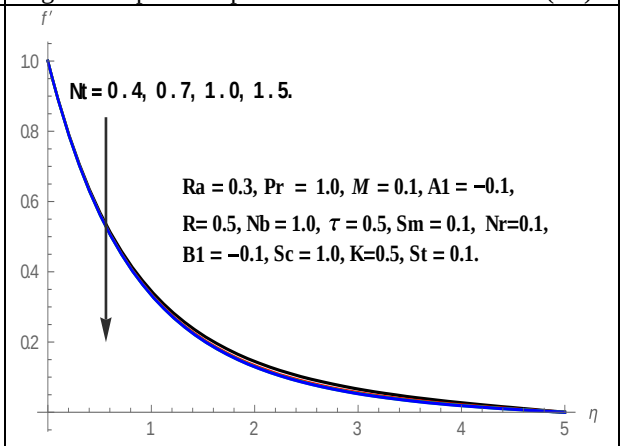

Fig.11. Velocity profiles for various values of (Nt)

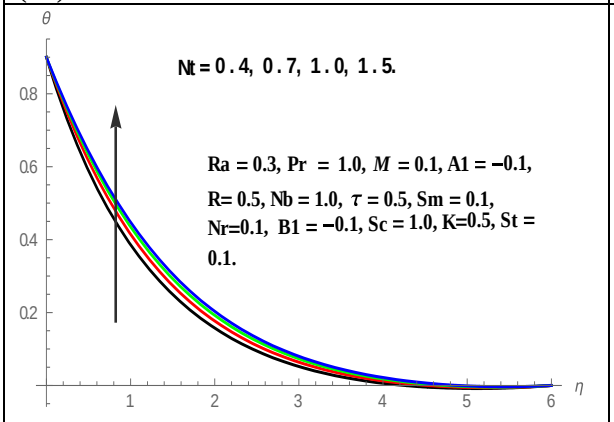

Fig.12.Temperature profiles for various values of (Nt)

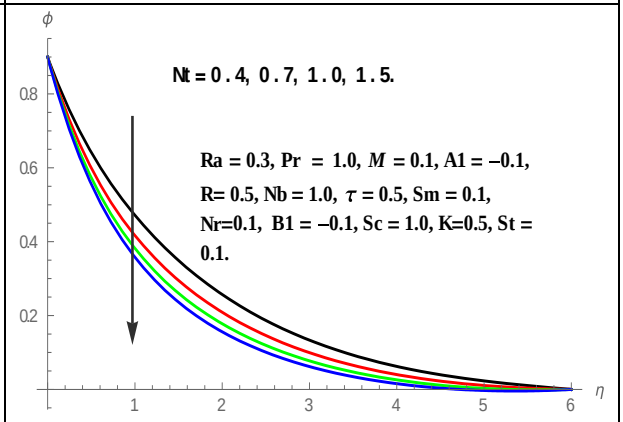

Fig.13. Concentration profiles for various values of (Nt)

Figs.8–10 display the impact ofmixed convection parameter (Ra) on velocity, temperature and concentration distributions. An increase in (Ra) elevates the momentum boundary layer thickness of the fluid (Fig. 8). It is analyzed that both temperature and concentration profiles decelerate with increasing values of (Ra) as shown in Fig. 9 & 10.

Variation in non-dimensional velocity, temperature and concentration distributions for different values of thermophoretic parameter (Nt) is depicted in Figs. 11 – 13. The thermophoresis acts against temperature gradient, so that, the particles move from the region of higher temperature to the region of lower temperature. The sketches of velocity diminishes in the boundary layer regime with growing values of (Nt) and is shown in Fig. 11. It is perceived from Fig. 12 that temperature profiles escalate in the boundary layer region with rising values of (Nt).

 https://doi.org/10.37896/pd93.4/93412

This is from the reality that particles near the hot surface create thermophoretic force; this force enhances the temperature of the fluid in the boundary layer region. However, the concentration distributions diminish as the values of (Nt) raises (Fig. 13).

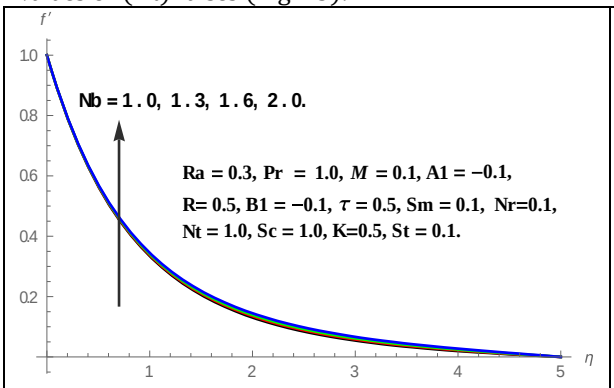

Fig.14.Velocity profiles for various values of (*Nb*)

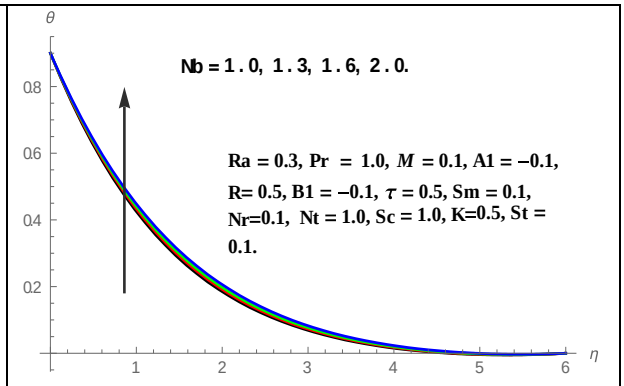

Fig.15.Temperature profiles for various values of (Nb)

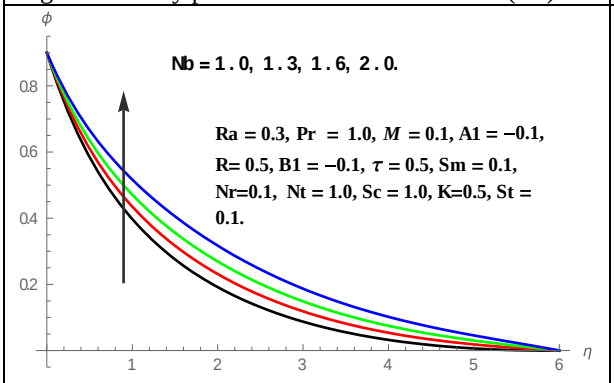

Fig.16.Concentration profiles for various values of (Nb)

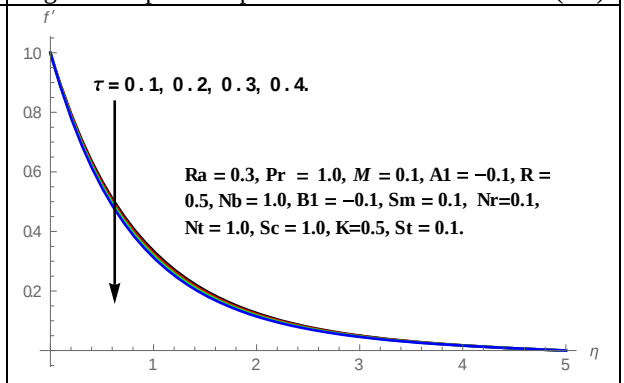

Fig.17.Velocity profiles for various values of (τ)

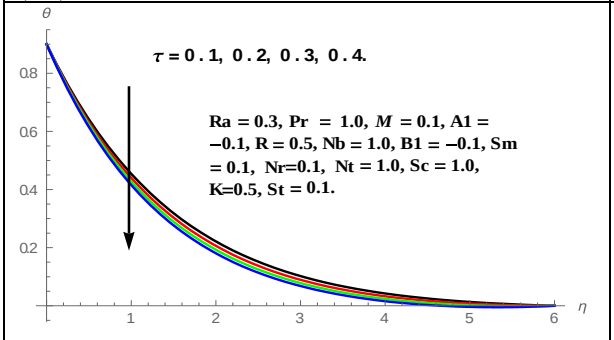

Fig.18.Temperature profiles for various values of (τ)

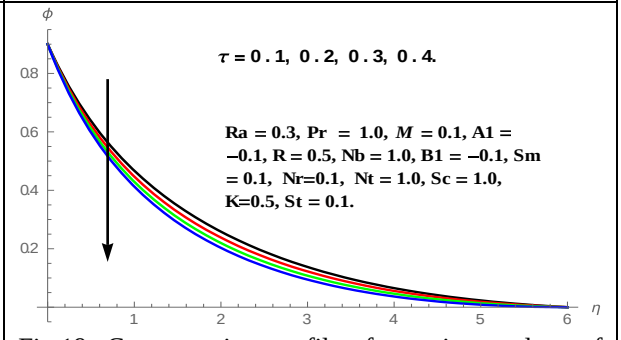

Fig.19. Concentration profiles for various values of (τ)

The effect of Brownian motion parameter (Nb) on velocity, temperature and concentration profiles is illustrated in Figs. 14 – 16. Brownian motion is the random motion of suspended nanoparticles in the base fluid and is more influenced by its fast moving atoms or molecules. It is noticed that with an increase in the values of (Nb) all profiles of velocity, temperature and concentration are enhanced in the entire fluid region. This is from the reality that the random motion of the particles improves when (Nb) values rises which causes an increment in kinematic energy as a result the fluid temperature grows.

The sway of unsteadiness parameter (τ) on velocity, temperature and concentration profiles is depicted in Figs. 17 – 19. It can be seen that velocity, temperature and concentration profiles are all decelerates with increase in the values of (τ). This is because of the usual fact that the motion is generated by the stretching of the sheet and the stretching sheet velocity and temperature is greater than the free stream velocity and temperature, so, the momentum, thermal and solutal boundary layer thickness decreases with increase in the values of (τ).

 https://doi.org/10.37896/pd93.4/93412

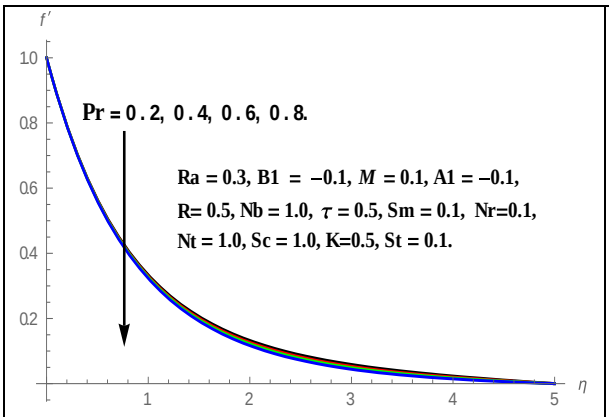

Fig.20.Velocity profiles for various values of (Pr)

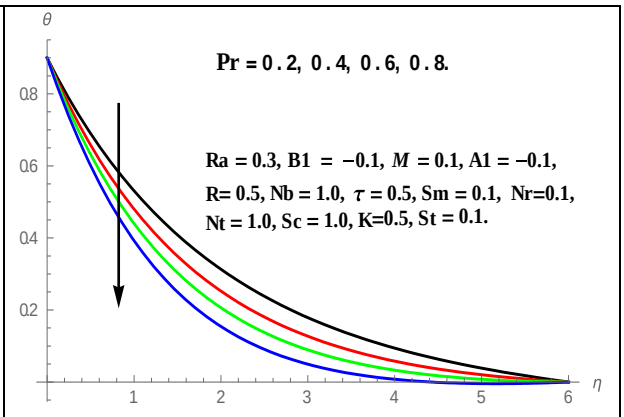

Fig.21.Temperature profiles for various values of (Pr)

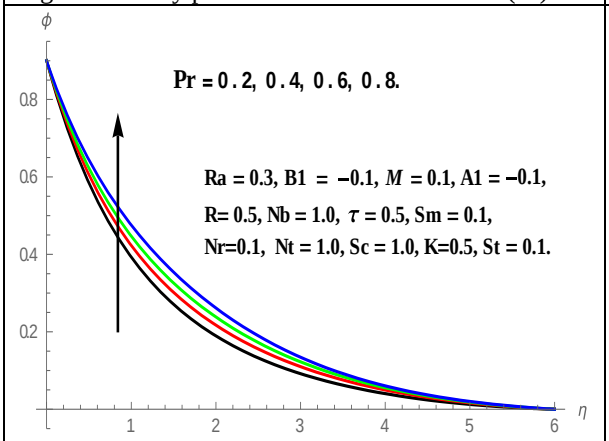

Fig.22.Concentration profiles for various values of (Pr)

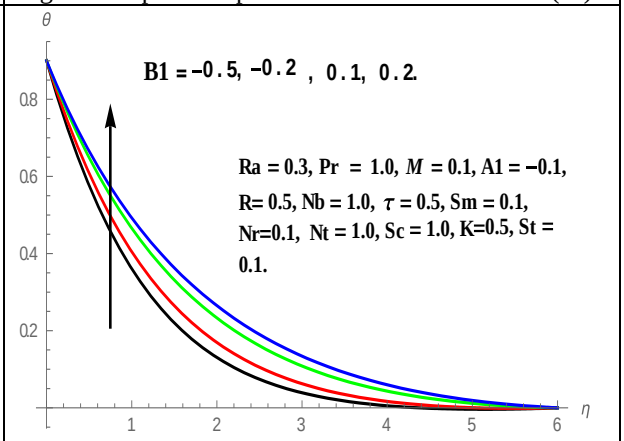

Fig.23.Temperature profiles for various values of (B1)

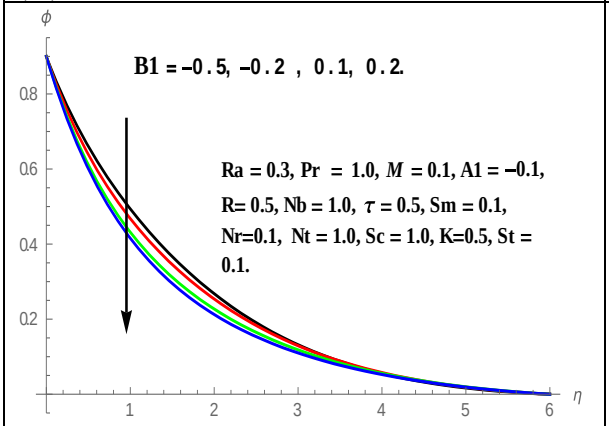

Fig.24. Concentration profiles for various values of (B1)

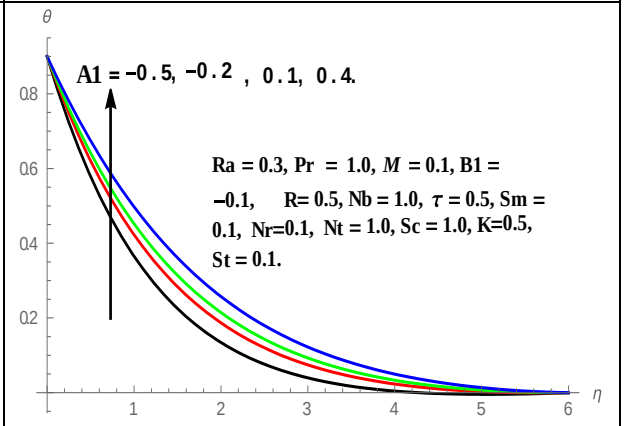

Fig.25.Temperature profiles for various values of (A1)

https://doi.org/10.37896/pd93.4/93412

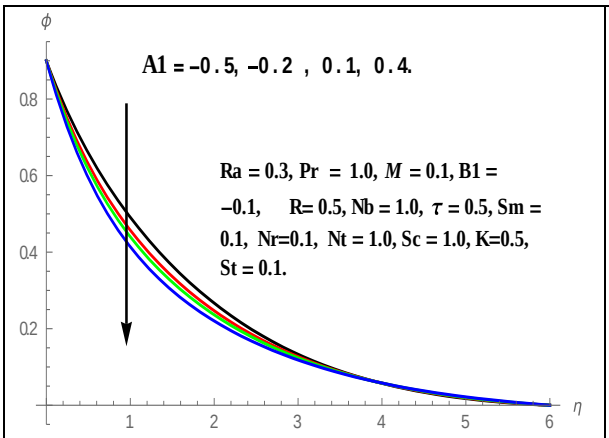

Fig.26. Concentration profiles for various values of (A1)

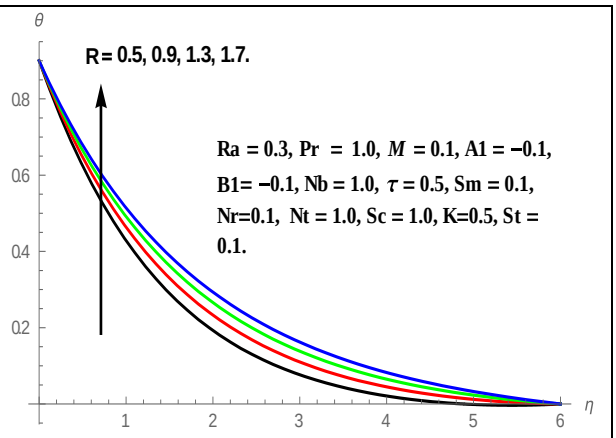

Fig.27. Temperature profiles for various values of (R)

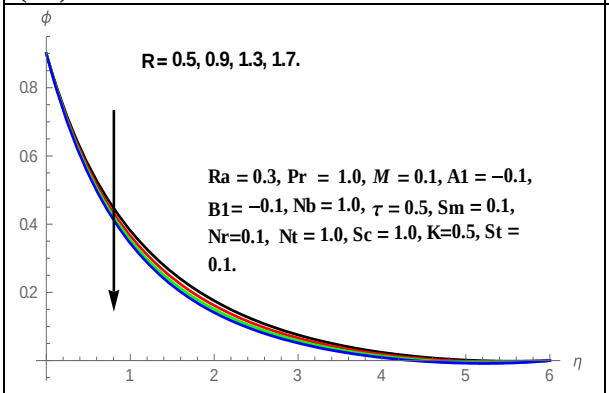

Fig.28. Concentration profiles for various values of (R)

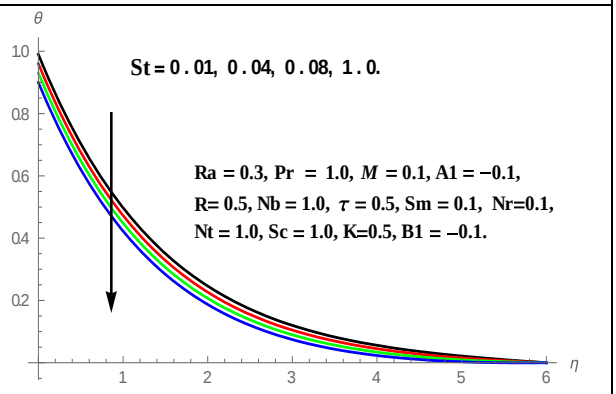

Fig.29. Temperature profiles for various values of (St)

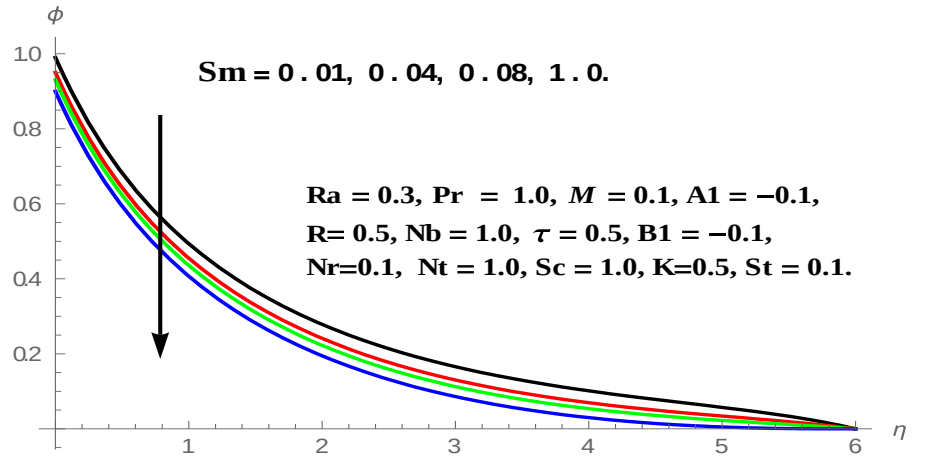

Fig.30. Concentration profiles for various values of (Sm).

The velocity, temperature and concentration distributions for various values of Prandtl number (Pr) are revealed in Figs. 20 – 22 respectively. It is reported that the velocity and temperature of the fluid depreciates as the values of (Pr) increases (Figs. 20 & 21). However, profiles of concentration intensifies with higher values of (Pr) (Fig. 22).

Variations in temperature and concentration profiles for different values of space – dependent(A1)and temperature dependent (B1)heat source/sink parameters are plotted in Figs. 23 – 26. It is perceived that the temperature of the fluid decelerates for both $A1 < 0, B1 < 0$ (sink), whereas, temperature of the fluid elevates for both $A1 > 0, B1 > 0$ (source). This is because of the fact that heat sink reduces the thickness of the thermal

https://doi.org/10.37896/pd93.4/93412

boundary layer, however, heat source elevates its thickness. Nevertheless, sketches of concentration are deteriorates with up surging values of (A1) and (B1).

The effect of radiation parameter (R) on temperature and concentration profiles is displayed in Figs. 27 – 28. It is perceived that the thermal boundary layer thickness is enhanced with the higher values of (R) in the entire flow region. This is due to the reality that (R) enhances the heat flux causes an increment in the temperature of the fluid (Fig. 27). However, there is a deceleration in the concentration boundary layer thickness with increasing values of (R) and is shown in Fig. 28.

Fig. 29 depicts the impact of thermal stratification point (St) on temperature profiles. It is noted that the thermal boundary layer thickness worsens with the higher values of (St). The temperature difference between the surface of the sheet and ambient fluid reduces as the values of (St) increase as a result the thickness of the thermal boundary layer is reduced. The nanoparticle concentration profiles depreciate with increasing values of (Sm) and are shown in Fig. 30.

Table 1. Comparison of Skin-friction coefficient C_f with previously published data when $K = 0, \tau = 0, R = 0, Ra = 0, Nr = 0, A = 0, B = 0, Sc = 0, St = 0, Sm = 0, Nb = 0, Nt = 0, Pr = 0$.

Parameter	C_f	
M	Ibrahim and Sankar [31]	Present Study
0	1.2808	1.2809
1	1.4142	1.4146
5	2.4494	2.4498

The non-dimensional rates of velocity, heat and mass transfer are also calculated and shown in tabular form. To check the validity of present numerical code, the results are compared with "Ibrahim et al. [32]." and are shown in Table 1.

Table 2. The values of Skin-friction coefficient$\left(f''(0)\right)$, Nusselt number $(-\theta'(0))$ and Sherwood number $(-S'(0)$) for different values of *M*, τ, Pr, R, Nt, Nb, Nr, Ra, St, Sm, A1, B1.

M	τ	Pr	R	Nt	Nb	Nr	Ra	St	Sm	A1	B1	$f''(0)$	$-\theta'(0)$	$-S'(0)$
0.1	0.5	1.0	0.5	1.0	1.0	0.1	0.3	0.1	0.1	-0.1	-0.1	1.21590	0.680527	0.792405
0.4	0.5	1.0	0.5	1.0	1.0	0.1	0.3	0.1	0.1	-0.1	-0.1	1.32430	0.671397	0.774938
0.7	0.5	1.0	0.5	1.0	1.0	0.1	0.3	0.1	0.1	-0.1	-0.1	1.46205	0.660335	0.754305
1.0	0.5	1.0	0.5	1.0	1.0	0.1	0.3	0.1	0.1	-0.1	-0.1	1.55809	0.652980	0.740918
0.5	0.1	1.0	0.5	1.0	1.0	0.1	0.3	0.1	0.1	-0.1	-0.1	1.15264	0.607951	0.666263
0.5	0.2	1.0	0.5	1.0	1.0	0.1	0.3	0.1	0.1	-0.1	-0.1	1.18619	0.632308	0.709313
0.5	0.3	1.0	0.5	1.0	1.0	0.1	0.3	0.1	0.1	-0.1	-0.1	1.21876	0.655443	0.749394
0.5	0.4	1.0	0.5	1.0	1.0	0.1	0.3	0.1	0.1	-0.1	-0.1	1.25042	0.677579	0.786723
0.5	0.5	0.2	0.5	1.0	1.0	0.1	0.3	0.1	0.1	-0.1	-0.1	1.17832	0.48521	0.81629
0.5	0.5	0.4	0.5	1.0	1.0	0.1	0.3	0.1	0.1	-0.1	-0.1	1.18274	0.56661	0.75729
0.5	0.5	0.6	0.5	1.0	1.0	0.1	0.3	0.1	0.1	-0.1	-0.1	1.18619	0.63230	0.70931
0.5	0.5	0.8	0.5	1.0	1.0	0.1	0.3	0.1	0.1	-0.1	-0.1	1.19019	0.71032	0.65202
0.5	0.5	1.0	0.5	1.0	1.0	0.1	0.3	0.1	0.1	-0.1	-0.1	1.28248	0.64861	0.86157
0.5	0.5	1.0	0.9	1.0	1.0	0.1	0.3	0.1	0.1	-0.1	-0.1	1.27888	0.59222	0.89237
0.5	0.5	1.0	1.3	1.0	1.0	0.1	0.3	0.1	0.1	-0.1	-0.1	1.27599	0.54739	0.91670
0.5	0.5	1.0	1.7	1.0	1.0	0.1	0.3	0.1	0.1	-0.1	-0.1	1.27362	0.51092	0.93637
0.5	0.5	1.0	0.5	0.4	1.0	0.1	0.3	0.1	0.1	-0.1	-0.1	1.17383	0.776196	0.129931

 https://doi.org/10.37896/pd93.4/93412

ISSN: 0369-8963

0.5	0.5	1.0	0.5	0.7	1.0	0.1	0.3	0.1	0.1	-0.1	-0.1	1.18647	0.670269	0.730720
0.5	0.5	1.0	0.5	1.0	1.0	0.1	0.3	0.1	0.1	-0.1	-0.1	1.18891	0.617466	0.894549
0.5	0.5	1.0	0.5	1.5	1.0	0.1	0.3	0.1	0.1	-0.1	-0.1	1.18911	0.588040	0.954809
0.5	0.5	1.0	0.5	1.0	1.0	0.1	0.3	0.1	0.1	-0.1	-0.1	1.18817	0.641132	0.831181
0.5	0.5	1.0	0.5	1.0	1.3	0.1	0.3	0.1	0.1	-0.1	-0.1	1.18402	0.621701	0.763920
0.5	0.5	1.0	0.5	1.0	1.6	0.1	0.3	0.1	0.1	-0.1	-0.1	1.18018	0.606582	0.699798
0.5	0.5	1.0	0.5	1.0	2.0	0.1	0.3	0.1	0.1	-0.1	-0.1	1.17543	0.592541	0.614498
0.5	0.5	1.0	0.5	1.0	1.0	0.1	0.3	0.1	0.1	-0.1	-0.1	1.28309	0.67426	0.77995
0.5	0.5	1.0	0.5	1.0	1.0	1.5	0.3	0.1	0.1	-0.1	-0.1	1.17051	0.68533	0.80234
0.5	0.5	1.0	0.5	1.0	1.0	3.0	0.3	0.1	0.1	-0.1	-0.1	1.05463	0.69580	0.82305
0.5	0.5	1.0	0.5	1.0	1.0	4.5	0.3	0.1	0.1	-0.1	-0.1	0.94260	0.70522	0.84132
0.5	0.5	1.0	0.5	1.0	1.0	0.1	0.5	0.1	0.1	-0.1	-0.1	1.32817	0.62897	0.80176
0.5	0.5	1.0	0.5	1.0	1.0	0.1	0.9	0.1	0.1	-0.1	-0.1	1.23568	0.63714	0.82156
0.5	0.5	1.0	0.5	1.0	1.0	0.1	1.3	0.1	0.1	-0.1	-0.1	1.14613	0.64452	0.83899
0.5	0.5	1.0	0.5	1.0	1.0	0.1	1.7	0.1	0.1	-0.1	-0.1	1.05897	0.65129	0.85466
0.5	0.5	1.0	0.5	1.0	1.0	0.1	0.3	0.01	0.1	-0.1	-0.1	1.17523	0.672556	0.697362
0.5	0.5	1.0	0.5	1.0	1.0	0.1	0.3	0.04	0.1	-0.1	-0.1	1.17937	0.668628	0.694409
0.5	0.5	1.0	0.5	1.0	1.0	0.1	0.3	0.08	0.1	-0.1	-0.1	1.18351	0.664665	0.691460
0.5	0.5	1.0	0.5	1.0	1.0	0.1	0.3	1.0	0.1	-0.1	-0.1	1.18766	0.660668	0.688516
0.5	0.5	1.0	0.5	1.0	1.0	0.1	0.3	0.1	0.01	-0.1	-0.1	1.27603	0.728589	0.806175
0.5	0.5	1.0	0.5	1.0	1.0	0.1	0.3	0.1	0.04	-0.1	-0.1	1.27890	0.728367	0.804372
0.5	0.5	1.0	0.5	1.0	1.0	0.1	0.3	0.1	0.08	-0.1	-0.1	1.28043	0.728255	0.803474
0.5	0.5	1.0	0.5	1.0	1.0	0.1	0.3	0.1	1.0	-0.1	-0.1	1.28250	0.728084	0.802128
0.5	0.5	1.0	0.5	1.0	1.0	0.1	0.3	0.1	0.1	-0.5	-0.1	1.19236	0.78077	0.59560
0.5	0.5	1.0	0.5	1.0	1.0	0.1	0.3	0.1	0.1	-0.2	-0.1	1.18766	0.66066	0.68851
0.5	0.5	1.0	0.5	1.0	1.0	0.1	0.3	0.1	0.1	0.1	-0.1	1.18523	0.59961	0.73549
0.5	0.5	1.0	0.5	1.0	1.0	0.1	0.3	0.1	0.1	0.4	-0.1	1.18148	0.50669	0.80666
0.5	0.5	1.0	0.5	1.0	1.0	0.1	0.3	0.1	0.1	-0.1	-0.5	1.19265	0.78122	0.59671
0.5	0.5	1.0	0.5	1.0	1.0	0.1	0.3	0.1	0.1	-0.1	-0.2	1.18912	0.69308	0.66421
0.5	0.5	1.0	0.5	1.0	1.0	0.1	0.3	0.1	0.1	-0.1	0.1	1.18406	0.58900	0.74104
0.5	0.5	1.0	0.5	1.0	1.0	0.1	0.3	0.1	0.1	-0.1	0.2	1.18175	0.54831	0.77002

5. Conclusion

It is found that the thermal stratification parameter (St) deteriorates the temperature of the liquid. The concentration of the liquid diminishes with rising values of solutal stratification number. The thermal limit layer breadth elevates with higher values of Brownian motion and thermophoresis numbers.

Nomenclature

g	Gravitational acceleration vector (m/s^2)
S_m	Mass stratification parameter
C	Nanoparticle volume fraction
C_∞	Ambient nanoparticle volume fraction

https://doi.org/10.37896/pd93.4/93412

T	Fluid temperature (K)
T_w	Temperature at the cone surface
T_∞	Ambient temperature attained
q_w	Wall heat flux
J_W	Wall mass flux
D_B	Brownian diffusion coefficient(m^2/s)
D_T	Thermophoretic diffusion coefficient(m^2/s)
$f(\eta)$	Dimensionless stream function
Nt	Thermophoresis parameter
P	Pressure (Pa)
K^*	Mean absorption coefficient
Ra	Mixed convention parameter
Nu_x	Nusselt number
C_w	Nanoparticle volume fraction on the cone
(x, y)	Cartesian coordinates
C,*D*	Constants
M	Magnetic parameter
A1, B1	Source/sink parameters
B_0	Magnetic field strength
R	Radiation parameter
Pr	Prandtl number

References:

[1] S.U.S. Choi, and J.A. Eastman, Enhancing Thermal Conductivity of Fluids with Nanoparticles, Proc. ASME Int. MechanicalEngineering Congress and Exposition, vol. 66, pp. 99–105, 1995.

[2] J.A. Eastman, S.U.S. Choi, S. Li, W. Yu, L.J. Thompson, Anomalously increased effective thermal conductivities of ethylene glycol-based nano-fluids containing copper nano-particles, Appl. Phys. 78 (2001) 718–720.

[3] J. Buongiorno., Convective transport in nanofluids, J Heat Transfer 128: (2006) 240–250.

[4] E. Abu-Nada, H.F. Oztop, Effects of inclination angle on natural convection in enclosures filled with Cu-water nanofluid, Int. J. Heat Fluid Flow, vol. 30,pp.669–678, 2009.

[5] A.V. Kuznetsov, and D.A. Nield, Natural convection boundary-layer of a nanofluid past a vertical plate, Int. J. Therm. Sci., vol. 49, pp.243–247, 2010.

[6] M.A.A. Hamad, Analytical solution of natural convection flow of a nanofluid over a linearly stretching sheet in the presence of magnetic field, International Communications in Heat and Mass Transfer, vol. 38, pp. 487–492, 2011.

[7] A. Noghrehabadi, R. Pourrajab, and M. Ghalambaz, Effect of partial slip boundary condition on the flow and heat transfer of nanofluids past stretching sheet prescribed constant wall temperature, International Journal of Thermal Sciences,vol. 54, 253 – 261, 2012.

[8] P. Rana, R. Bhargava, Flow and heat transfer of a nanofluid over a nonlinearly stretching sheet: a numerical study, Comm. Nonlinear Sci. Numer. Simulat.,17 (2012) 212– 226.

[9] A. Noghrehabadi, R. Pourrajab, and M. Ghalambaz, Flow and heat transfer of nanofluids over stretching sheet taking into account partial slip and thermal convective boundary conditions, Heat Mass Transf.,vol.49, pp.1357–1366, 2013.

[10] A.J. Chamkha, A.M. Rashad, Ch. RamReddy and P.V. Murthy, Effect of suction/injection on free convection along a vertical plate in a nanofluid saturated non-Darcy porous medium with internal heat generation,Indian Journal of Pure and Applied Mathematics,vol. 45, pp. 321-341, 2014.

[11] M.M. Rashidi, N.V. Ganesh, A.K.A. Hakeem and B. Ganga, Buoyancy effect on MHD flow of nanofluid over a stretching sheet in the presence of thermal radiation, J. Mol. Liq,vol.198, pp. 234–238, 2014.

[12] M. Sheikholeslami, R. Ellahi, H.R. Ashorynejad, G. Domairry and T. Hayat, Effects of heat transfer in flow of nanofluids over a permeable stretching wall in a porous medium, Journal of Computational and Theoretical Nanoscience,vol.11, pp. 486-496, 2014.

[13] S.A. Mansur, A. Ishak and I. Pop, Three-dimensional flow and heat transfer past a permeable exponentially stretching/shrinking sheet in a nanofluid, Journal of Applied Mathematics 517273, http://dx.doi.org/10.1155/2014/517273., 2014.

[14] A. Zaraki, M. Ghalambaz and A.J. Chamkha, Mehdi Ghalambaz, Danilo De Rossi, Theoretical analysis of natural convection boundary layer heat and mass transfer of nanofluids: Effects of size, shape and type of

nanoparticles, type of base fluid and working temperature, Advanced Powder Technology, vol. 26, pp. 935–946, 2015.
[15] H. Zargartalebi, M. Ghalambaz, A. Noghrehabadi and A.J. Chamkha, Stagnation-point heat transfer of nanofluids toward stretching sheets with variable thermo-physical properties, Advanced Powder Technology, vol. 26, pp. 819–829, 2015.
[16] M.A. Sheremet, T. Grosan, and I. Pop, Free convection in a square cavity filled with a porous medium saturated by nanofluid using Tiwari and Das'nanofluid model, Transp. Porous Media, vol. 106pp. 595–610, 2015.
[17] M.A. Ismael, T. Armaghani and Ali.J. Chamkha, Conjugate heat transfer and entropy generation in a cavity filled with a nanofluid-saturated porous media and heated by a triangular solid, Journal of the Taiwan Institute of Chemical Engineers,vol. 59, 138 – 151, 2015.
[18] Y. Raja Obula Reddy, M. Suryanarayana reddy, P.sudarsana Reddy and Ali.J. Chamkha, Effect of Brownian motion and Thermophoresis on heat and mass transfer flow over a horizontal circular cylinder filled with nanofluid, Journal of Nanofluids, vol.6,702-710, 2017.
[19] T. Hayat, K. Muhammad, A.Farooq, A. Alsaedi,Melting Heat Transfer in Stagnation Point Flow of Carbon Nanotubes towards Variable Thickness Surface,AIP ADVANCES, vol.6,pp. 015214,2016.
[20] N. Bachok, A. Ishak and I. Pop, Unsteady Boundary-Layer Flow and Heat Transfer of a Nanofluid Over a Permeable Stretching/Shrinking Sheet, Int. J. Heat Mass Transfer, vol. 55, 2102–2109, 2012.
[21] S. Khalili, S. Dinarvand, R. Hosseini, H. Tamim, and I. Pop, Unsteady MHD flow and heat transfer near stagnation point over a stretching/shrinking sheet in porous medium filled with a nanofluid, Chin. Phys. B, vol.23, 048203,2014.
[22] O.D. Makinde and M.S. Tshehla, Unsteady hydromagnetic flow of radiating fluid past a convectively heated vertical plate with the navier slip, Advances in Mathematical Physics (2014) 973593, http://dx.doi.org/10.1155/2014/973593.
[23] K. Das, P.R. Duari, and P.K. Kundu, Effects of magnetic field on an unsteady mixed convection flow of nanofluids containing spherical and cylindrical nanoparticles, Journal of Heat Transfer, vol.138, pp. 061901 – 1, 2016.
[24] I. Pop, S.P. Mohamed Isa, Norihan, M. Arifin, RoslindaNazar, NorfifahBachok, and M.Ali. Fadzilah, Unsteady viscous MHD flow over a permeable curved stretching/shrinking sheet, International Journal of Numerical Methods for Heat & Fluid Flow, vol. 26, pp. 2370 – 2392, 2016.
[25] Ahmada Omar Ali, Oluwole Daniel Makinde, Yaw Nkansah-Gyekye, Numerical study of unsteady MHD Couette flow and heat transfer of nanofluids in a rotating system with convective cooling, International Journal of Numerical Methods for Heat & Fluid Flow,Vol. 26, pp. 1567 – 1579, 2016.
[26] T. Hayat, K. Muhammad, A.Farooq, A. Alsaedi,Melting Heat Transfer in Stagnation Point Flow of Carbon Nanotubes towards Variable Thickness Surface,AIP ADVANCES, vol.6,pp. 015214,2016.
[27] PuneetRana, R. Bhargava, O.A. Bég, Numerical solution for mixed convection boundary layer flow of a nanofluid along an inclined plate embedded in a porous medium, Computers and Mathematics with Applications, vol. 64, pp.2816–2832, 2012.
[28] P. Sudarsana Reddy, A.J. Chamkha, Soret and Dufour effects on MHD heat and mass transfer flow of a micropolar fluid with thermophoresis particle deposition, Journal of Naval Architechure and Marine Engineering 13 (2016) 39-50.
[29] P. Sudarsana Reddy and A.J. Chamkha, Influence of size, shape, type of nanoparticles, type and temperature of the base fluid on natural convection MHD of nanofluids, Alexandria Eng. J,vol. 55, 331-341, 2016.
[30] P. Sudarsana Reddy, P. Sreedevi, A.J. Chamkha, MHD boundary layer flow, heat and mass transfer analysis over a rotating disk through porous medium saturated by Cu-water and Ag-water nanofluid with chemical reaction, Powder Technology. 307 (2017) 46 – 55.
[31] W. Ibrahim and B. Shankar, MHD boundary layer flow heat transfer of a nanofluid past a permeable stretching sheet with velocity thermal and solutal slip boundary conditions, Comput. Fluids,vol.75pp. 1–10, 2013.
[32] W. Ibrahim and O.D. Makinde, The effect of double stratification on boundary layer flow and heat transfer of nanofluid over a vertical plate, Comput. Fluids, vol. 86, pp. 433–441, 2013.